

Design and Drop-Test Analysis of Paddle Wheel Mechanisms for Rotation in Microgravity Environments

Calder Russell · Thomas Ang

Abstract

This study evaluated two novel paddle wheel mechanisms within a controlled free-fall environment to explore maximum rotational motion under microgravity. The primary objective was to determine whether water-surface interactions, enhanced through hydrophobic treatments, could generate sufficient torque to initiate and sustain wheel rotation. Two distinct paddle wheel designs, one traditional and one spiral-inspired, were fabricated using PLA. Parts of these paddles were sprayed with a hydrophobic coating to assist in the propulsion of the paddle in microgravity. Despite rigorous testing in a custom-built drop chamber simulating microgravity, neither wheel achieved significant sustained rotation. Observed angular displacements were minimal and inconsistent, with one design exhibiting transient motion limited to $\sim 15^\circ$. Analysis suggests that interfacial forces

alone were insufficient to overcome axle friction and rotational inertia, even with extended free-fall duration. These findings highlight critical design challenges, including the need for enhanced initial torque generation and reduced mechanical resistance. Future work should focus on optimizing blade asymmetry, minimizing friction via bearings or a similar mechanism, and exploring active mechanisms to enable continued rotation in microgravity environments. This research contributes to the broader understanding of mechanical behavior in microgravity and informs future innovations in aerospace engineering and fluid-interactive systems.

1. Introduction

This research sought to evaluate two innovative paddle wheel mechanisms integrated within a free-fall experimental module. The primary goal was to investigate whether rotational motion could be initiated

under drop conditions, potentially enabling novel methods for energy conversion and passive stabilization. Despite expectations, the experimental findings indicated a complete absence of rotation in the paddle wheel, prompting a deeper inquiry into the underlying dynamics, such as aerodynamic drag, frictional forces, and the influence of microgravity on mechanical systems. This experiment not only aimed to address fundamental questions in rotational dynamics but also to explore applications that extend beyond the challenge itself. A functioning paddle wheel system could, for example, serve as an efficient energy-harvesting component during re-entry or descent, contribute to advanced control systems in spacecraft, and inform the design of mechanical components resilient to extreme conditions. Additionally, insights from this study have broader implications for terrestrial engineering challenges, ranging from the optimization of renewable energy devices in variable fluid environments to the development of low-maintenance mechanical actuators for industrial applications. By examining both the experimental shortcomings and potential breakthroughs, this work contributes to the evolving dialogue on sustainable and innovative engineering solutions in aerospace and related fields.

2. Materials

The paddles were constructed using a 3D printer in PLA. PLA, or polylactic acid, is the most commonly used plastic used for 3d printing. The material is easy to use and is quite suitable for light usage outside of hot temperatures. PLA can, however, absorb water if left alone too long. In order to mediate this, a base coat was needed. Base Coat: Grey served as protection for each plastic paddle, making sure they would be protected from the aquatic environment and would not absorb water. Rust-Oleum Multi-Surface NeverWet (Liquid Repelling Treatment) was chosen as a hydrophobic coating. Testing on a variety of materials with and without the base coat as well as the top coat led us to the conclusion that this treatment was extremely effective in creating hydrophobic surfaces. Rust-Oleum Multi-Surface NeverWet Top Coat solidified the base coatings on the paddles making sure the intended effects of each coating were kept effective. Additionally in order to perform the tests that were done a drop chamber was constructed. A drop chamber can be made using a plastic box able to be watertight, an axel must be mounted on one wall and the camera (highspeed) on the other wall. The chamber must then be filled

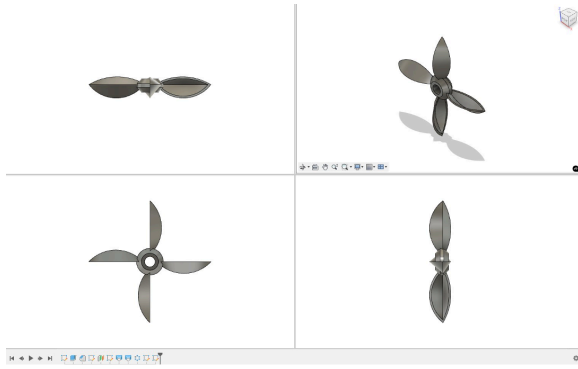


Fig. 1. Orthographic Image of Paddle Wheel 1

with water to the desired level for paddle wheel performance.

3. Methods

The first step in creating each paddle was conducting research and brainstorming ideas for both form and function. A set of criteria was established to guide design. Number of blades, blade rotation, shape, and paddle weight were identified as key factors to prioritize (Carlton, 2019). It soon became evident that the paddles were not designed to generate propulsion, but rather to be driven by it. Rather than optimizing the propulsion of the paddle itself, the design was shifted to improving how water propels the paddle, essentially reversing the approach. To do this, the paddle designs needed to focus on minimizing hub vortex, and wake disturbance, factors that limit the movement of the propeller due to opposing force. (Yin, 2023). Many of these factors were not due to size or weight, but how the propeller spins in water. In microgravity, the

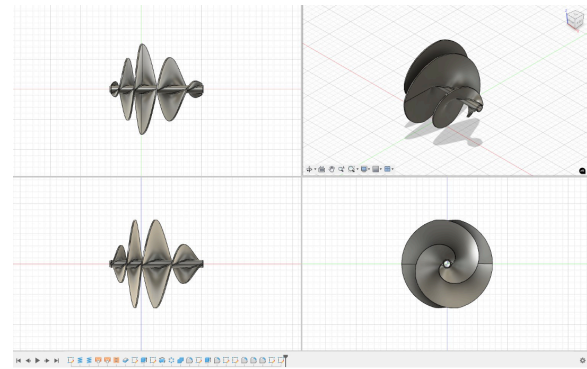


Fig. 2. Orthographic Image of Paddle Wheel 2

absence of gravity leads to surface tension becoming the dominant force in fluid behavior. This shift affects fluid-solid interactions, which are crucial for mechanisms like paddle wheels that rely on fluid contact to generate torque (Ungar, 2021). This led us to focus on designing sleeker paddles that could cut through the water as efficiently as possible. These paddles had to be extremely easy to spin, as the interaction between hydrophobic surfaces should facilitate the rotation. Fusion 360 was used to 3D model and iterate on the paddle designs. Two distinct approaches were taken: one paddle wheel followed a more traditional design, while the other drew inspiration from spiral wind turbine structures. The more traditional design was an asymmetrical thin paddle design utilizing an offset center point on each paddle in order to increase surface area on one side as much as possible. In addition to this, a shallow divot inside each blade was created

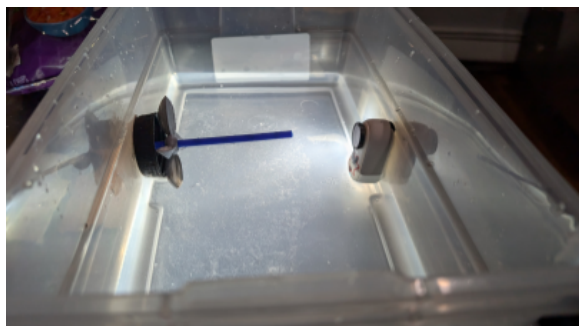


Fig. 3. Image of First Test setup

which was coated for hydrophobicity to propel the paddle. The Archimedes Spiral Wind Turbine seemed like it might have some promise; this design had been applied in wind turbine farms as an effective means of generating energy (Jang, 2019). Due to its large surface area strong hydrophobic forces could be implemented on this paddle. A drop chamber was also necessary to conduct the microgravity testing on the paddles. A sealed container sized to house the hydrophobic PLA paddle wheels and shallow (25 mm) water bath was engineered (BREUNINGER). A custom 3D-printed bracket and low-friction axle assembly used within the container emphasized rigid structural alignment to minimize mechanical disturbance (BREUNINGER). During Test one the paddles were initially tested in Microgravity by being dropped 7 meters. The paddles were in freefall for 1.195 seconds. The maximum water height during testing was set to 25 mm. This would allow for the paddles to interact with the water but not be stopped by



Fig. 4. Image of First Test Inside Box view

the water while attempting to spin, and to reduce the likelihood of water pinning to the axle or leaking through the axle holes. The paddles were mounted on an axle parallel to the surface of the water as seen in figures 3 and 4. Water fill: The chamber was filled to the target depth (25 mm for Drop 1; 22-23 mm for Drop 2) and level verified with a digital caliper. Mounting: The prepared

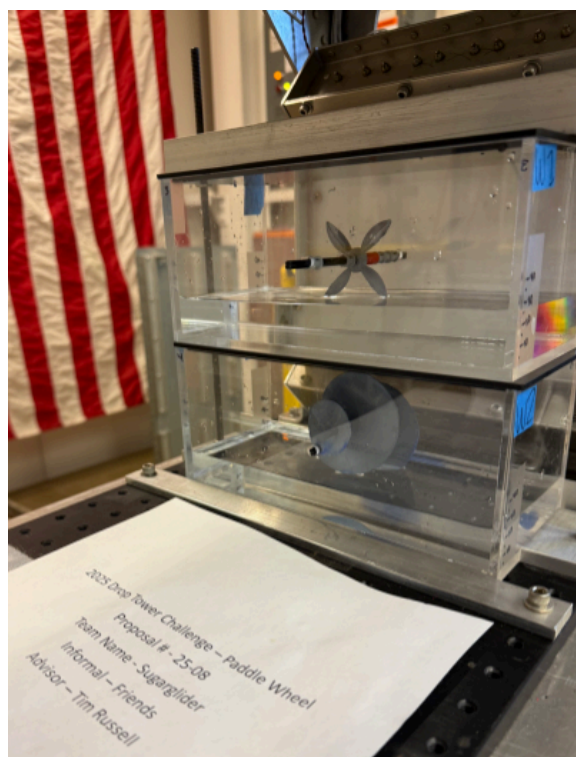


Fig. 5. Image of the Second Test Setup

wheel was slid onto the axle, and its starting angular position was recorded. Recording: A high-speed video camera (≥ 120 fps) was focused on the wheel; ambient lighting was held constant. Release: The drop module was released, yielding a free-fall duration of ~ 1.195 s. Recovery: After impact, the module was retrieved. During Test Two, the paddles were tested in Microgravity by being dropped 24m; The paddles were in freefall for 2.2 seconds. To ensure that the conditions were as similar as possible for the paddles in each drop, a stacked system was created that was used for both paddles (Fig. 5). The maximum water height during testing was set to 35 mm. This would allow for the paddles to interact with the water more fully and achieve greater results. The paddles were mounted on an axle parallel to the surface of the water. This test was conducted in a drop tower with a much more controlled environment; the results from this test are generally much more reliable, yielding clearer, more consistent data. Water fill: The

chamber was filled to the target depth (35 mm for Drop 1; 20-22 mm for Drop 2), and the level was verified with a digital caliper. Mounting: The prepared wheel was slid onto the axle, and its starting angular position was recorded. Additionally, an endcap was used to stop the Wheels from falling off as they did during Test 1. Recording: A video camera was focused on the wheel; ambient lighting was held constant. Release: The drop module was released, yielding a free-fall duration of ~ 2.2 s. Recovery: After impact, the module was retrieved.

5. Results

Below are several images and tables illustrating the testing conducted on the paddle designs:

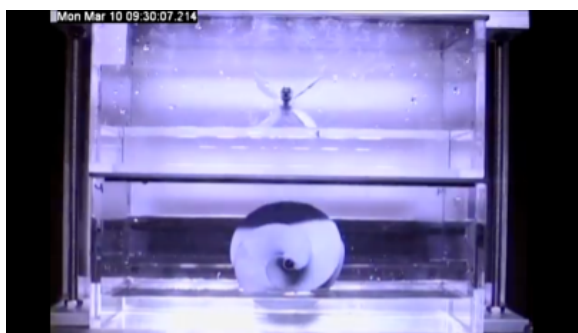


Fig. 6. Starting image of Drop 1 Test 2

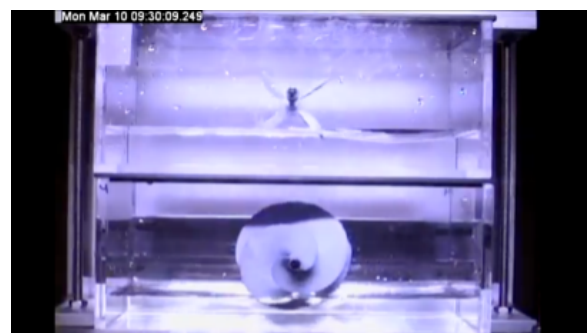


Fig. 7. Ending image of Drop 1 Test 2

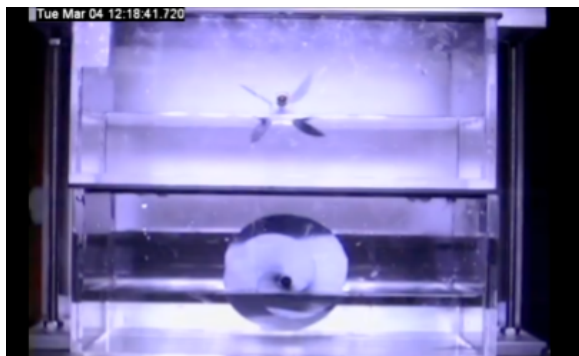


Fig. 8. Starting image of Drop 2 Test 2

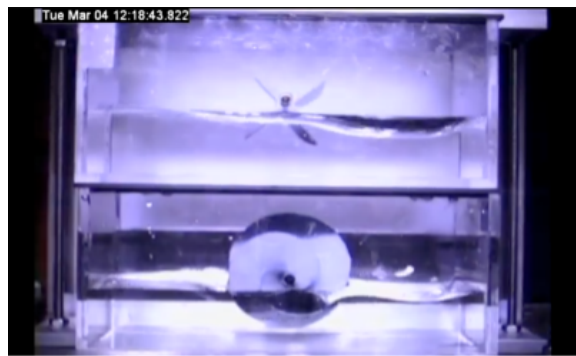


Fig. 9. Ending image of Drop 2 Test 2

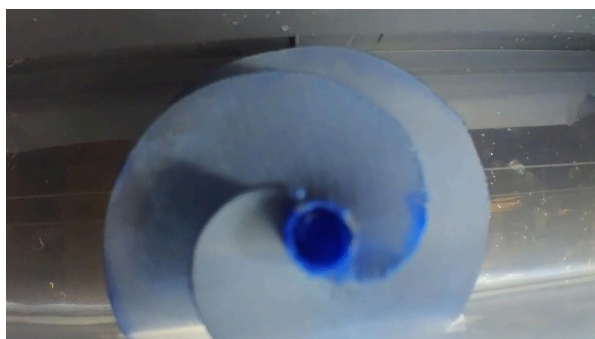


Fig. 10. Starting image of Drop 2 Test 1



Fig. 11. Ending image of Drop 2 Test 1

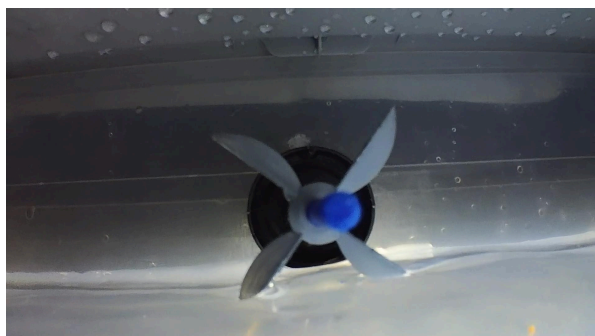


Fig. 12. Ending image of Drop 2 Test 1



Fig. 13. Ending image of Drop 2 Test 1

Table 1. Rotation of Paddle Wheels and Water depth for Test 1

Wheel & Drop	Initial Water Depth (mm)	Angular Displacement (°)
Wheel 1 – Drop 1	25	180 CW
Wheel 1 – Drop 2	22	Failed (fell off axel)
Wheel 2 – Drop 1	25	10 CCW
Wheel 2 – Drop 2	23	170 CCW

6. Discussion

Despite the hypothesis, Wheel 2 (spiral design) exhibited zero measurable rotation during the more controlled test (Test 2), and Wheel 1 showed only minor rotation (<15°) only in the first drop of Test 2. Throughout the design and fabrication process, the focus of each paddle was overly concentrated on the paddle's interaction with water, rather than on the optimal shaping and placement of hydrophobic surfaces to maximize propulsion. By creating paddles that would cut through water most effectively, properties that would inhibit the paddle's rotational effectiveness were overlooked. Another issue that was failed to consider was

Table 2. Rotation of Paddle Wheels and Water depth for Test 2

Wheel & Drop	Initial Water Depth (mm)	Angular Displacement (°)
Wheel 1 – Drop 1	35	15 CW(Clockwise)
Wheel 1 – Drop 2	22	2 CCW (Counter Clockwise)
Wheel 2 – Drop 1	35	0
Wheel 2 – Drop 2	20	0

friction. Even minimal axle friction under microgravity requires substantial interfacial torque to overcome. For example, Wheel 2 had a relatively large mass and long hole/hub, suggesting that under microgravity conditions, a greater force would have been required to initiate its rotation. A larger or heavier wheel requires more interfacial force to initiate movement, and without gravity to press fluid against blades, fluid-surface interaction is too weak to overcome resistance. However, initial assumptions were made that in microgravity, the mass of the wheel would be less significant, provided that a sufficient force could be applied to initiate rotation. Wheel 1 did not have the same issue of mass as

Wheel 2, though only minimal rotation on Drop 1 was seen and little to no rotation on Drop 2. This likely occurred because the designs were too focused on sustaining paddle rotation in microgravity, rather than on developing an initial rotation during the transition from gravity to microgravity. Instead, focusing on generating an initial rotation and sustaining it through the use of hydrophobic surfaces seems to be a potential solution (Ungar, 2021). To improve rotation initiation, future designs should maximize continuous hydrophobic contrast around the circumference, further minimize friction, and consider alternative fluids with lower surface tension. In order to develop a design that can achieve this, a slightly asymmetrical paddle design could be developed, one that leverages the transition from gravity to microgravity by directing force downward on one side of the paddle to initiate rotation.

7. Conclusion

In the second drop test (2.2 seconds free-fall), neither paddle wheel achieved sustained rotation: Wheel 1 had shown up to $\sim 15^\circ$ of motion, and exhibited only a small angular deflection early in the extended drop before stalling completely, while Wheel 2 remained stationary throughout. This result demonstrates that hydrophobic/hydrophilic

interfacial forces generated only a transient torque that is rapidly dissipated by bearing friction, axle drag, and surface-tension pinning, such that even doubling the microgravity interval produces no additional acceleration or cumulative rotation. Moreover, both wheels' relatively large moment of inertia means that once the initial impulse is expended, insufficient continuous torque remains to overcome mechanical losses. Consequently, extending microgravity duration alone does not compensate for these fundamental barriers. To achieve reliable paddle wheel rotation in space applications, future designs must either incorporate mechanisms for continuous or periodically reinforced torque, such as pulsatile surface interactions or active fields, or drastically reduce mechanical losses through innovations like magnetic-levitation bearings or superhydrophobic continuous coatings (Flemming, 1991). Alternative approaches, including lower-viscosity fluids, blade geometries that trap and release fluid pockets, and adjustable preload systems, should also be explored to determine whether any purely passive configuration can generate and sustain the interfacial forces necessary to overcome inertia and friction under extended microgravity (Hu et al. 2024).

References

- BREUNINGER, Jakob & BELSER, Valentin & Laufer, Rene & Dropmann, Michael & Herdrich, Georg & Hyde, Truell & RÖSER, Hans-Peter. (2016). Design of a 1.5 Seconds High Quality Microgravity Drop Tower Facility. TRANSACTIONS OF THE JAPAN SOCIETY FOR AERONAUTICAL AND SPACE SCIENCES, AEROSPACE TECHNOLOGY JAPAN. 14. Ph_7-Ph_14. 10.2322/tastj.14.Ph_7
- Carlton, J. S. (2019). *Marine Propellers and Propulsion (Fourth Edition) - Propeller Design*. ScienceDirect. Retrieved October 3rd, 2024, from <https://www.sciencedirect.com/topics/engineering/propeller-design>
- Fleming, D. P. (1991, July). Magnetic bearings—State of the art (NASA Technical Memorandum 104465). National Aeronautics and Space Administration, Lewis Research Center. <https://ntrs.nasa.gov/api/citations/19910016099/downloads/19910016099.pdf>
- H, J. (2019). Analysis of Archimedes Spiral Wind Turbine Performance by Simulation and Field Test. *Energies*, 12(24), 4624. <https://doi.org/10.3390/en12244624>
- Hu, J., Xu, Y., Chen, P., Xie, F., Li, H., & He, K. (2024). Design and Reality-Based Modeling Optimization of a Flexible Passive Joint Paddle for Swimming Robots. *Biomimetics* (Basel, Switzerland), 9(1), 56. <https://doi.org/10.3390/biomimetics9010056>
- Jang, H., Kim, D., Hwang, Y., Paek, I., Kim, S., & Baek, J. (2019). Analysis of Archimedes Spiral Wind Turbine Performance by Simulation and Field Test. *Energies*, 12(24), 4624. <https://doi.org/10.3390/en12244624>
- Ungar, E. K. (2021, August 25). Two-phase behavior in microgravity (NASA Technical Report No. 20210018162). NASA Technical Reports Server. <https://ntrs.nasa.gov/citations/20210018162>
- Yin, C. (2023, January 23). *Improve Ship Propeller Efficiency via Optimum Design of Propeller Boss Cap Fins*. MDPI. Retrieved April 5, 2025, from <https://www.mdpi.com/1996-1073/16/3/1247>